Jinst

Published by IOP Publishing for Sissa Medialab

Received: *June 27, 2019*
Revised: *November 7, 2019*
Accepted: *November 25, 2019*
Published: *January 10, 2020*

3rd European Conference on Plasma Diagnostics (ECPD2019)
6–10 May 2019
Lisbon, Portugal

Conceptual design of JT-60SA edge Thomson scattering diagnostic

R. Pasqualotto,[a,g,1] H. Tojo,[b] A. Fassina,[a] L. Giudicotti,[a] V. Nardino,[c] N. Oyama,[b] S. Pelli,[c] V. Raimondi,[c] S. Ricciarini,[c] S. Soare,[d,e] S. Davis[f] and C. Sozzi[g]

[a] *Consorzio RFX, C.so Stati Uniti 4, Padova 35127, Italy*

[b] *National Institutes for Quantum and Radiological Science and Technology (QST), 801-1 Mukoyama, Naka 311-0193, Japan*

[c] *National Research Council, Institute of Applied Physics "Nello Carrara" (CNR-IFAC), via Madonna del Piano 10, 50019 Sesto Fiorentino, Italy*

[d] *Institute of Atomic Physics, 407 Atomistilor St., Magurele 077125, Ilfov, Romania*

[e] *Universitatea "Lucian Blaga" Sibiu, 10 Bld. Victoriei, Sibiu 55002, Romania*

[f] *Fusion for Energy (F4E), Boltzmannstrasse 2, Garching 85748, Germany*

[g] *National Research Council, Institute for Plasma Science and Technology (CNR-ISTP), via R.Cozzi 53, Milano 20125, Italy*

E-mail: roberto.pasqualotto@igi.cnr.it

Abstract: JT-60SA will complement ITER in resolving key issues to finally decide an acceptable DEMO design. Diagnostics play a key role in this mission. The electron temperature and density profiles are measured by a core and an edge Thomson scattering (TS) diagnostics with high spatial resolution, needed to identify the pedestal parameters and small profile structures. The two systems use a common tangential Nd:YAG laser beam path in the plasma equatorial plane. The collection optics for the edge system (low field side) is hosted in a lower oblique port and that for the core system in a horizontal port. The optics fit in the port plug tube and image the scattering volumes into an array of fiber bundles. They both are exposed to a high neutron dose of 10^{16} n/cm^2 over 13 years of operation. The optics are supported by a mechanical structure decoupled from the cryostat. A set of filter polychromators with avalanche photodiode (APD) detectors spectrally analyze the

[1] Corresponding author.

https://doi.org/10.1088/1748-0221/15/01/C01011

scattered radiation. The development of the TS systems is carried out by a joint Japan-EU team. The conceptual design of the edge TS system is presented here. Simulations of the TS signals show acceptable accuracy down to $1 \times 10^{19}\ \mathrm{m}^{-3}$ electron density, sufficient to measure the edge gradient and even a small region outside the separatrix.

Keywords: Plasma diagnostics - interferometry, spectroscopy and imaging; Optics; Photon detectors for UV, visible and IR photons (solid-state) (PIN diodes, APDs, Si-PMTs, G-APDs, CCDs, EBCCDs, EMCCDs, CMOS imagers, etc); Spectrometers

Contents

1 Thomson scattering systems in JT-60SA

The mission of the JT-60SA superconducting tokamak (maximum plasma current I_p = 5.5 MA, major radius $R_p \sim 3$ m, plasma volume $V_p \sim 130\,\text{m}^3$, aspect ratio $A \sim 2.6$, single and double null configurations) is to complement ITER in resolving key physics and engineering issues to finally decide an acceptable DEMO plasma design [1]. To this purpose diagnostics play a key role. The electron temperature T_e and density n_e profiles will be measured by two Thomson scattering (TS) systems under development. A system is dedicated to the core plasma (P2), the other one to the low field side outer plasma region including outside the last closed flux surface (P1), while a third one covering the high field side (P5) is planned in the future (figure 1). They will be characterized by a high spatial resolution, required to identify the pedestal parameters (expected width is < 50 mm)

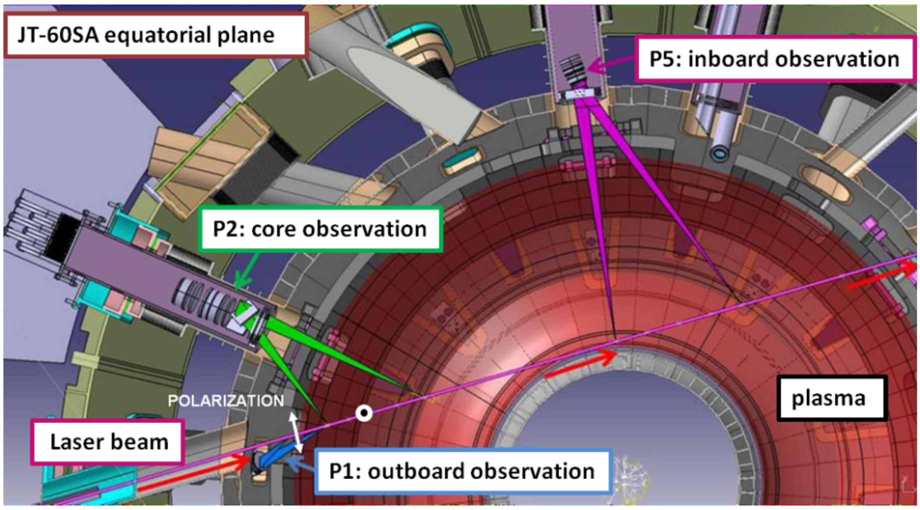

Figure 1. Equatorial section of the JT-60SA tokamak with collection optics and radial coverage of three TS systems: P1-low field side (blue) looking from a lower port, P2-core (green) and P5-high field side (purple) from equatorial ports. Also shown is the common path of the TS laser beams (purple) entering the vessel from the left and passing tangential to the inner wall: the required beam polarizations for P1 and P2 are respectively horizontal and vertical.

2020 JINST 15 C01011

Table 1. Design specifications of the core (P2) and edge (P1) TS systems. The scattering volume length is the fiber bundle image projection on the laser beam path, without aberrations.

	Core TS	**Edge TS**
Major radius coverage	46 points in R = 2.60–3.73 m	50 points in R = 3.70–4.17 m
Scattering volume length	15 mm	5.5 mm
Radial resolution	25 mm	25–10–5.5 mm (core → edge)
T_e dynamic range, @ $n_e > 1 \times 10^{-19}$ m^{-3}	0.1–30 keV	0.01–10 keV
Laser pulse repetition rate	50 Hz	100 Hz

and small profile structures. Specifications of P1 and P2 are reported in table 1. All TS systems share the same 1064 nm Nd:YAG laser beam path, passing the torus equatorial plane tangentially to the inner wall and exiting the vessel towards an external beam dump.

2 Layout of the edge Thomson scattering system

The edge system is based on a proven conventional incoherent TS setup with a pulsed Nd:YAG laser and filter polychromators [2, 3]. Its design has been driven by two main issues. The critical alignment conditions are caused by the 50m beam path which is sensitive to vibrations caused by disruptions, during plasma start-up and other sources. The other issue is the small space envelope for the collection optics and its orientation. Assessments of T_e and n_e accuracies using design parameters to ensure the target performance are reported in section 3.

The edge TS collection optics are installed at the end of a port plug attached to a cryostat flange, looking upward. The port plug is mechanically decoupled from the vacuum vessel and inner wall, so that vibrations are not directly transmitted (figure 2). Optics are positioned just behind the

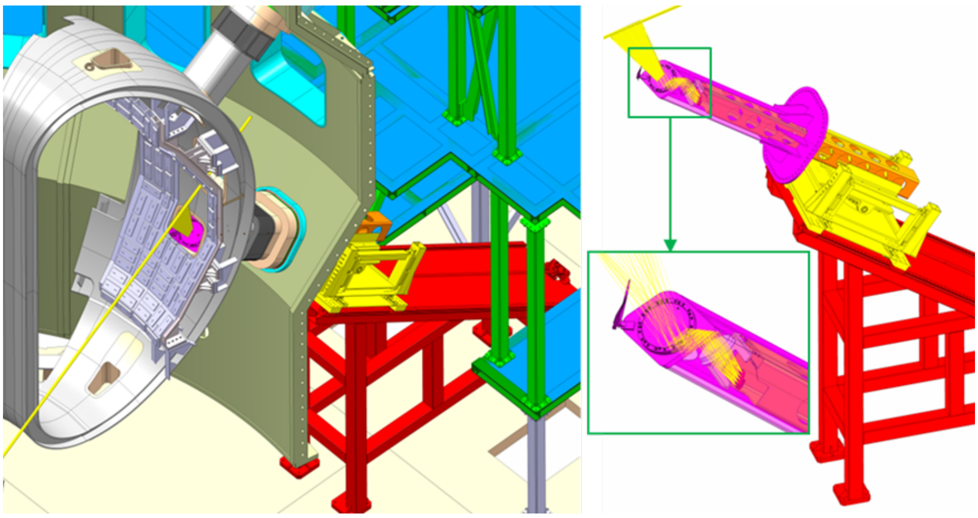

Figure 2. Layout of edge TS collection optics: vertical section of cryostat, vacuum vessel and first wall showing the 4.5 m tall support structure (red), standing on the floor, the 2.2 m long port plug ending with the vacuum window (purple), the laser beam and lines of sight (yellow). The yellow trolley sliding on the ramp holds the retractable arm (orange) supporting the collection optics.

2020 JINST 15 C01011

vacuum window protected by a cover glass in vacuum (figure 3). They are attached to a retractable arm that is held and inserted inside the port plug tube by a trolley which slides on an oblique ramp completely supported from the floor, thus decoupling the optics and all its supports from the cryostat (figure 2). The same trolley is also used to install the port plug.

The collection optics, evolving from the design in [4], are made of two doublets with a couple of steering mirrors in between. This allows tilting the optical axis both vertically and horizontally for the optics to fit inside the port plug within the limited inner cross section of 420 mm width and 380 mm height. Scattering angles are in the range 113°–129°. Scattering volumes of 5.5 mm length and about 13 mm width across the beam, allowing ±2.5 mm alignment tolerance against vibrations, are imaged onto bundles of 200 µm core diameter fiber optics, with ~ 3.7 demagnification at the optical axis. The up to $F/9$ collection efficiency, with maximum 180 mm clear aperture, fits the 0.22 NA of the fibers. Fiber bundles are contiguous in the outer region, but more apart towards the plasma core (figure 3).

Since a total neutron dose of 10^{16} n/cm^2 is expected for 13 years operation, radiation resistant glasses for the four lenses and fluorine doped silica-silica fibers have been selected. High transmission in the 660–1064 nm detected spectral range, required to cover the 10 eV–10 keV T_e range, asks for fibers containing a low concentration of OH, which are less radiation tolerant than fibers with high OH content: intermediate OH content (2–30 ppm) will be specified as a compromise solution. However, the radiation induced absorption will be significant only below about 700 nm, thus affecting only the innermost positions with $T_e > 2$ keV.

Two pairs of alignment fiber bundles are positioned, as shown in figure 3, one after the innermost position, the other sufficiently apart towards the edge but at a position with high enough n_e, to monitor the collection optics alignment looking at the TS or Raman signal ratio in each pair [5]. The fiber bundles holder will have remotely controlled adjustments to correct its image position and tilt across the laser beam.

Each fiber bundle, 80–90 m long, is routed inside the diagnostic room to a polychromator, based on interference filters and APDs. The 660–1064 nm TS spectrum is detected into 5 spectral

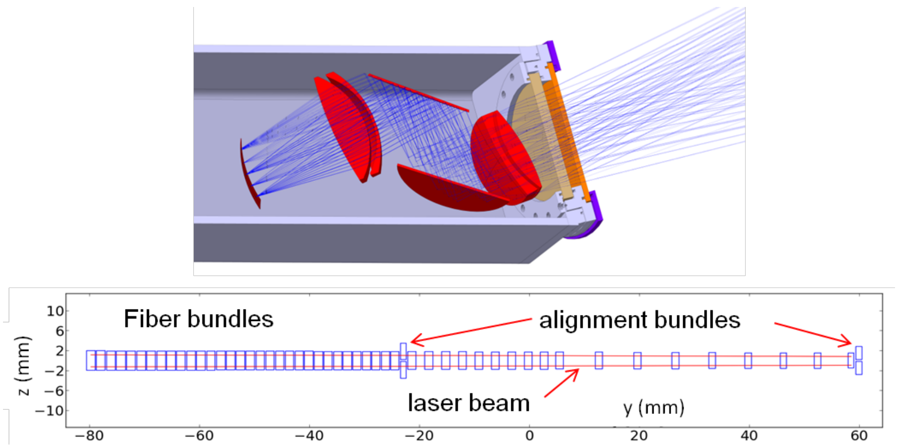

Figure 3. Top: vertical cross section of the port plug (grey) with the vacuum window (brown) flange including the in-vacuum absorbing glass (orange) and of the collection optics with the curved image surface (red). Bottom: layout of the fiber optic bundles

2020 JINST 15 C01011

channels. A sixth one, centered on the 1064 nm laser line and 3 nm wide, is reserved for Rayleigh scattering calibration. Suggested channel sensitivities and spectral intervals are shown in figure 4. The total 96 polychromators including both the core and edge measurements will be hosted in 6 cubicles in the diagnostic room. The acquisition system sitting nearby is made of digitizer boards on a VME bus (IEEE-1014-1987) with 32 channels, 12 bit, 1 GS/s. Each channel samples about 1 μs trace for each laser pulse, so that the 1 GB on board memory can locally store the data of the entire plasma discharge. The background plasma light can be separately sampled over the plasma pulse with slower digitizers.

A 3 J, 100 Hz Nd:YAG laser, with about 10 ns FWHM pulse duration, will be dedicated to the edge TS system and its beam will be overlapped to that of the core TS, with orthogonal polarization, inside the diagnostic room. The two beams will share the full beam path up to the external beam dump [6]. External trigger of individual pulses will allow synchronization with the laser pulses of the core TS system and occasionally with plasma events.

3 Performance simulation

The expected signal levels of the edge TS system at given values of T_e and n_e have been analytically derived using the key parameters described above. T_e and n_e relative errors have then been calculated from the photoelectron statistics, the plasma background light variation and the detector noise [2, 7]. Assuming an injected laser energy of 2.75 J, central scattering volume with 121° scattering angle and $F/11$ collection angle, 5.5 mm scattering length, 0.7 and 0.4 transmission of collection optics and fiber bundles respectively, and the spectral sensitivities in figure 4, the results derived for n_e = 1×10^{19} m^{-3}, lower bound of the usually expected densities, are also shown in the figure. At least three channels have significant signal level in the entire required T_e range, except below 40 eV where

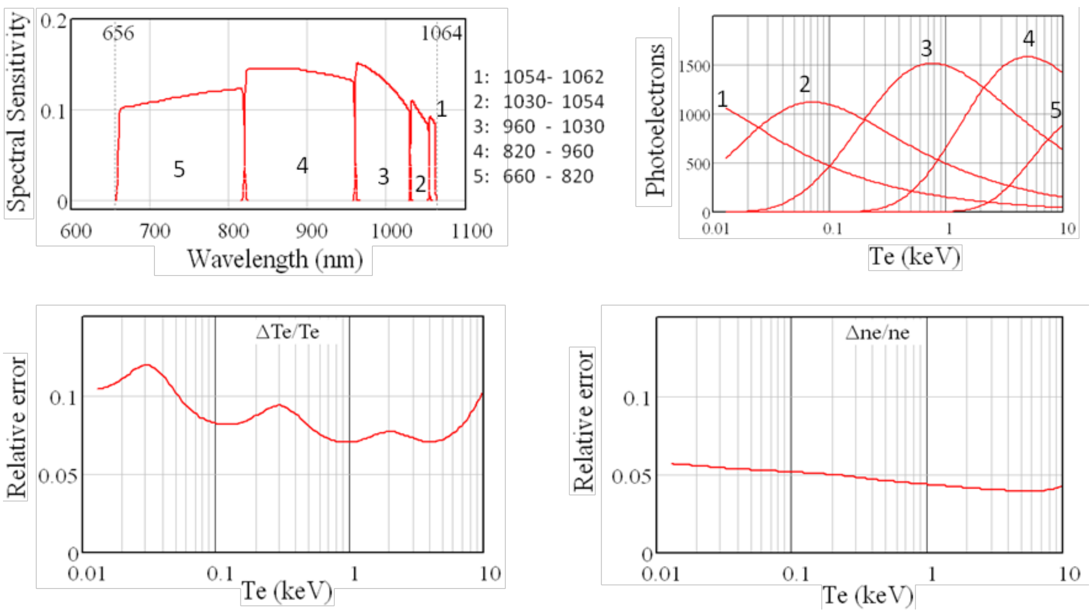

Figure 4. Top: spectral sensitivity of the polychromator channels with wavelength range (left) and the expected signal level at $n_e = 1 \times 10^{19}$ m^{-3} (right). Bottom: predicted relative error of T_e (left) and n_e (right).

only two channels are effective. The relative error, including only shot noise and APD dark noise equivalent to 30 photoelectrons with an excess noise factor of 4, is $< 12\%$ for T_e and $< 6\%$ for n_e.

Accuracy over the full profiles has been calculated taking into account the noise contribution from the background plasma light, calculated from the bremsstrahlung spectral emissivity over the line of sight with a $\times 2$ enhancement factor to include line radiation [7]. Results for a specific plasma scenario and with the designed parameters are shown in figure 5. In agreement with figure 4, the relative errors appear stable and low inside R = 4.13 m, where $n_e > 1 \times 10^{19}\ \mathrm{m}^{-3}$, while they diverge outside, where n_e is lower. Most of the pedestal gradient of both T_e and n_e profiles falls inside the measurable region and it is then measured with sufficient accuracy and number of points, allowing evaluation of its shape. Specific simulations of the edge profiles indicate $n_e > 1\times 10^{19}\ \mathrm{m}^{-3}$ up to 1 cm outside the separatrix, where low $T_e < 50$ eV are expected (figure 6). For this reason the dynamic range of the diagnostic has been extended downwards to 10 eV. These results also indicate that the collection optics, though limited in aperture by the available space, still collect sufficient light.

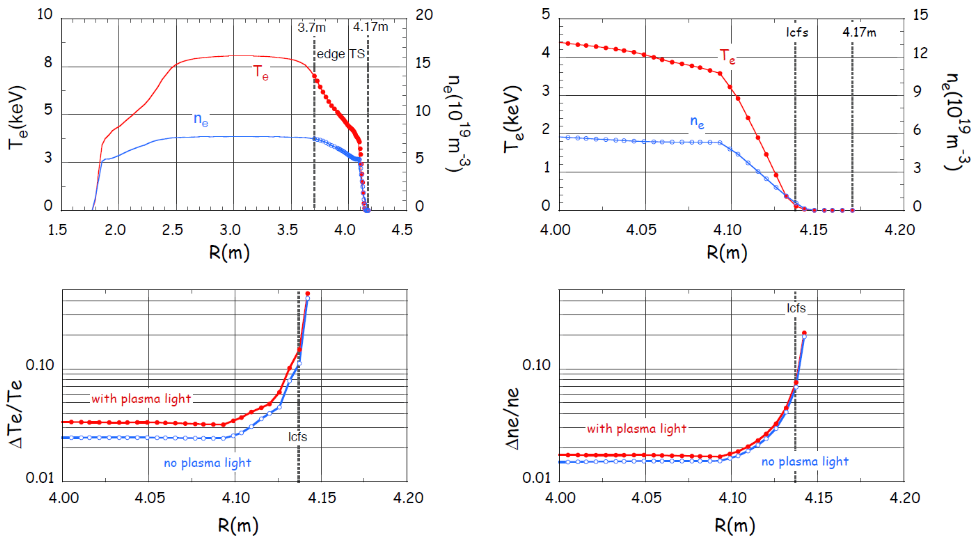

Figure 5. Top: full T_e and n_e profiles (left) of the scenario "inductive H-mode low density" [8], with edge TS spatial coverage (dashed lines) and positions (circles); zoom (right) on the pedestal region $R = 4.0$–4.2 m, lcfs: last closed flux surface @ $R = 4.137$ m. Bottom: predicted relative error of T_e (left) and n_e (right), with (red) and without (blue) plasma light expected error contribution.

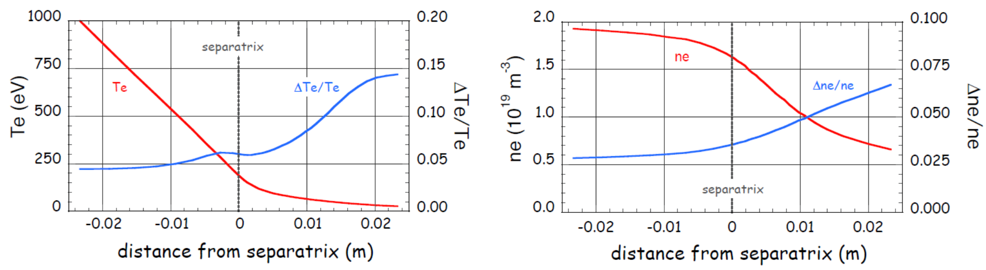

Figure 6. T_e (left) and n_e (right) profiles at the separatrix, modeled using the SONIC code [9], with relative errors.

2020 JINST 15 C01011

An issue to be considered is that in plasma scenarios with upper single null or double null [10, 11], strong plasma-wall interaction occurs at the upper divertor plates. They are in direct view of the collection optics for the innermost measured positions $R = 3.7$–$4.0\,\mathrm{m}$, which will be blinded by the intense plasma background light. In most configurations however the pedestal will be outside $R = 4.0\,\mathrm{m}$, thus T_e and n_e measurements will be unaffected there and pedestal parameters can still be evaluated.

4 Outlook

A future option is a double-pass TS, which takes advantage of the external beam dump, replaceable with a mirror [12, 13]. Independently measuring the incident and reflected laser pulses, the double measurement can be used to increase accuracy, especially at the high T_e values, because the spectrum from the return beam is narrower, or to monitor online the spectral sensitivity in a self-calibrating arrangement.

2020 JINST 15 C01011

Acknowledgments

This work has been carried out within the framework of the EUROfusion Consortium and has received funding from the EURATOM research and training programme 2014–2018 and 2019–2020 under grant agreement No 633053. The views and opinions expressed herein do not necessarily reflect those of the European Commission. The authors gratefully acknowledge members of the JT-60SA Integrated Project Team for data exchange and fruitful discussions.

References

[1] Y. Kamada et al., *Progress of the JT-60SA project*, *Nucl. Fusion* **53** (2013) 104010.

[2] R. Pasqualotto et al., *High resolution Thomson scattering for Joint European Torus (JET)*, *Rev. Sci. Instrum.* **75** (2004) 3892.

[3] R. Scannell et al., *A 130 point Nd:YAG Thomson scattering diagnostic on MAST*, *Rev. Sci. Instrum.* **81** (2010) 10D520.

[4] H. Tojo et al., *An optical design and accuracy estimation for a JT-60SA edge Thomson scattering diagnostic*, 2013 *JINST* **8** C12025.

[5] H. Yoshida et al., *Quantitative method for precise, quick, and reliable alignment of collection object fields in the JT-60U Thomson scattering diagnostic*, Rev. Sci. Instrum. **68** (1997) 1152.

[6] H. Tojo et al., *Conceptual design of laser transfer system of the JT-60SA Thomson scattering diagnostic*, *Fusion Eng. Des.* **123** (2017) 678.

[7] L. Giudicotti, *Polarimetric Thomson scattering for high Te fusion plasmas*, 2017 *JINST* **12** C11002.

[8] J. Garcia et al., *Physics comparison and modelling of the JET and JT-60U core and edge: towards JT-60SA predictions*, *Nucl. Fusion* **54** (2014) 093010.

[9] H. Kawashima et al., *Development of Integrated SOL/Divertor Code and Simulation Study in JAEA*, *Plasma Fusion Res.* **1** (2006) 031.

[10] Yong Guo et al., *A divertor plasma configuration design method for tokamaks*, *Chin. Phys.* **B 25** (2016) 115201.

[11] G. Giruzzi et al., *Advances in the physics studies for the JT-60SA tokamak exploitation and research plan*, *Plasma Phys. Control. Fusion* **62** (2020) 014009.

[12] H. Tojo et al., *First measurement of electron temperature from signal ratios in a double-pass Thomson scattering system*, *Rev. Sci. Instrum.* **83** (2012) 023507.

[13] L. Giudicotti, R. Pasqualotto and A. Fassina, *Dual-angle, self-calibrating, Thomson scattering measurements in RFX-MOD*, *Rev. Sci. Instrum.* **85** (2014) 11D823.